Transmission Dynamics of and Insights from the 2018-2019 Measles Outbreak in New York City: A Modeling Study

Wan Yang (wy2202@columbia.edu)

Department of Epidemiology, Mailman School of Public Health, Columbia University, NY, NY

Abstract:

In 2018-2019, New York City experienced the largest measles outbreak in the US in nearly three decades. To identify key factors contributing to this outbreak to aid future public health interventions, here we developed a model-inference system to infer the transmission dynamics of measles in the affected community, based on incidence data. Our results indicate that delayed vaccination of young children aged 1-4 years enabled the initial spread of measles and that increased infectious contact among this age group, likely via gatherings intended to expose unvaccinated children (i.e. "measles parties"), further aggravated the outbreak and led to widespread of measles beyond this age group. We found that around half of infants were susceptible to measles by age 1 (the age-limit to receive the first vaccine dose in the US); as such, infants experienced a large number of infections during the outbreak. We showed that without the implemented vaccination campaigns, the outbreak severity including numbers of infections and hospitalizations would be 10 times higher and predominantly affect infants and children under 4. These results suggest that recommending the first vaccine dose before age 1 and the second dose before age 4 could allow pro-vaccine parents to vaccinate and protect infants and young children more effectively, should high level of vaccine hesitancy persist. In addition, enhanced public health education is needed to reduce activities that unnecessarily expose children to measles and other infections.

Introduction

Measles is highly contagious and severe viral disease. Thanks to a highly effective vaccine and high coverage of vaccination, endemic transmission of measles—i.e. continuous transmission for more than 12 months—in the US was declared eliminated in 2000. However, due to vaccine hesitancy and declining vaccination rate, in recent years there have been an increasing number of large outbreaks following introduction of measles infection (*1*). Due to long-term fluctuations in vaccine coverage and infection history, population susceptibility could vary substantially by age group. This susceptibility disparity by age can further interact with age-specific social connectivity (i.e., contact rate) to shape the epidemic trajectory. As such, understanding these detailed population characteristics as well as their impact on transmission dynamics in the recent outbreaks is important for devising timely and effective intervention strategies.

In the fall of 2018, several New York City (NYC) residents acquired measles while traveling abroad and subsequently led to the largest measles outbreak in the US in nearly three decades. The first case of this outbreak developed a rash on Sep 30, 2018 and as of Aug 6, 2019 (at the time of this writing), there have been 642 confirmed cases, largely occurring in an Orthodox Jewish community (*2, 3*). To contain the outbreak, the NYC Department of Health and Mental Hygiene (DOHMH) launched extensive vaccination campaigns and, on Apr 9, 2019, ordered mandatary vaccination of all individuals living, working or going to school in the affected zip codes. As a result, over 32 thousand individuals under 19 years were vaccinated with the measles, mumps, and rubella (MMR) vaccine during Oct 2018 – July 2019 and the outbreak subsided (*3, 4*).

In this study, we model the transmission dynamics of this measles outbreak in the affected Orthodox Jewish community in NYC from Oct 1, 2018 to July 31, 2019, months with more than one measles cases reported. Using an age-structured model-inference framework, we are able to estimate key epidemiological features including the initial susceptibilities in five different age groups (i.e., <1, 1-4, 5-17, 18-49, and 50+ years) and the basic reproductive number R_0, infer key factors contributing to the spread of measles, estimate the proportions of infection attributable to each age group, as well as assess the impact of vaccination campaigns. We also discuss the implications of our findings to current measles vaccination policies.

Results

Overview of the measles outbreak and model fit

The measles outbreak started on Sep 30, 2018, when a young child developed a rash. It evolved relatively slowly in the first three months; however, the outbreak took off quickly in early 2019, peaked in April after the city declaring a public health emergence, and recorded a total of 642 cases by July 31, 2019. As shown in Fig. 1, age-grouped incidence, estimated based on health reports/alerts (*3, 5*), peaked first in Mar 2019 among 1-4 year-olds—the age group with the largest number of infection (275 cases or 42.8% of the total, as of Aug 6, 2018), followed by <1 year-olds (100 cases or 15.6%) and 5-17 year-olds (138 cases or 21.5%) in Apr 2019, and 18+ year-olds (129 cases or 20.1%) in May 2019.

As shown in Fig. 2 and Table S2, our model-filter system was able to recreate the overall incidence curve during Oct 2018 – July 2019, estimate the overall age distribution of measles cases, as well as recreate the estimated age-grouped incidence curves for all age groups. Note

70 that while our model (Eqn 1) divided 18+ year-olds into two subgroups (i.e. 18-49 and 50+
71 years) given their differences in contact rates and interactions with other age-groups, we present
72 the combined results here because data were only available for the entire age group. The
73 estimated reporting rate was around 90% throughout the study period and slightly lower in Apr
74 2019, at the peak of the outbreak [89.1%, 95% credible interval (CI): 79.4, 99.2%; Fig. S2].
75
76 *Inference of key epidemiological characteristics*
77 The model-filter system estimated that, at the beginning of the outbreak (i.e. Sep 2018),
78 susceptibility was the highest in infants, at approximately 53.2% (95% CI: 49.0, 57.5%; Fig.
79 3A). This was expected, because maternal immunity wanes within 3 to 9 months after birth and,
80 as a result, by their first birthday—the age eligible to receive the first dose of MMR vaccine in
81 the US—almost all infants have lost their maternal immunity and are susceptible to measles.
82 Young children aged 1-4 years had the second highest susceptibility; approximately 24.9% (95%
83 CI: 20.4, 29.7%) were susceptible. In comparison, susceptibility was lower among both 5-17
84 year-olds (6.0%, 95% CI: 4.1, 7.9%) and 18+ year-olds 6.0% (95% CI: 4.4, 7.6%; Fig. 3). These
85 estimates were consistent with the observation that all cases recorded in Oct 2018 were children
86 ranging from 11 months to 4 years (*2*). Sensitivity analysis on assumptions related to the
87 vaccination campaigns showed that estimated susceptibilities were slightly higher for 5-18 year-
88 olds (7.5%, 95% CI: 5.1, 9.9%) and 18-49 year-olds (7.9%, 95% CI: 5.2, 9.9%) if more vaccine
89 doses were given to the Jewish Orthodox community or 5-18 year-olds; however, the estimates
90 were in general consistent with the baseline scenario (Table S2).
91

92 The initial vaccination campaigns launched promptly afterwards lowered the
93 susceptibility to 40.3% (95% CI: 36.4, 44.0%) in infants and 13.9% (95%: 9.7, 18.7%) in 1-4
94 year-olds, by the end of Dec 2018 (Fig. 3). These efforts along with other transmission and
95 infection controls (*2*) appeared to effectively contain the outbreak at the time. The effective
96 reproductive number (R_e) is a key epidemiological parameter reflecting the potential of an
97 infection to cause an epidemic in a partially immune population; an epidemic is possible when
98 R_e>1. The estimated R_e was 1.5 (95% CI: 0.7, 2.9) in Oct 2018 and dropped to round 1 (95% CI:
99 0.7, 1.5) in Dec 2018 (Fig. 4B).
100
101 The outbreak, however, took off again in early 2019 (Fig. 1). The estimated R_e increased
102 and remained above 1 in the first three months of 2019 (Fig. 4B). In a perfectly mixed model, R_e
103 is computed as the product of the basic reproductive number R_0 and population susceptibility. In
104 particular, the basic reproductive number R_0 measures the transmissibility of an infection in a
105 fully susceptible population; for measles, while often reported in the range of 12-18, R_0 could
106 vary from 1.4 to 770 (*6*). In this study, we estimated that R_0 was approximately 7 during the
107 entire outbreak (Fig. 4A). Population susceptibility, the other factor for R_e, were to increase in a
108 close population (i.e., without migration), could only do so slowly as infants lose maternal
109 immunity. Thus, these two factors alone could not explain the sudden large increase in R_e (Fig.
110 4B). In this study, we utilized an age-structured model that enables more detailed analysis of the
111 transmission dynamics. Indeed, our model-filter system detected an increase in contact rate
112 among 1-4 year-olds during Jan-March 2019 (Fig. 4D); this increased contact rate along with the
113 high susceptibility among 1-4 year-olds appeared to raise R_e above unity (Eqn 5 in Methods) and
114 contribute to the re-surge of measles in early 2019. This finding was also consistent with reports

115 of parents hosting "measles parties" to exposure unvaccinated children at the time (*7*). In
116 contrast, estimated contact rates were relatively stable for other age groups (e.g., Fig. 4 E and F
117 for 5-17 and 18-49 year-olds, respectively). As a result, infections increased quickly among 1-4
118 year-olds (Figures 1 and 4D), reaching a peak of around 80 cases in March. Meanwhile,
119 infections also increased in other age groups including 5-17 and 18+ year-olds despite their low
120 overall susceptibilities, due to interactions between age-groups (Fig. S2) and the high contact
121 rates in these groups (Fig. 4 E and F).
122
123 The outbreak began to decline in Apr 2019, following more stringent public health
124 interventions (*3, 4*). In particular, the model estimated that, thanks to extensive vaccination
125 campaigns, susceptibility was reduced to 22.8% (95% CI: 19.3, 26.0%) in <1 year-olds, 4.3%
126 (95% CI: 0.5, 8.9%) in 1-4 year-olds, and 2.4% (95% CI: 0.4, 4.4%) in 5-17 year-olds at the end
127 of May. Consequently, the effective reproductive number R_e dropped below 1 from April
128 onwards.
129
130 *Who acquired infection from whom?*
131 Table 1 shows the estimated proportions of infections caused by each of the five age groups
132 based on the estimated Who-Acquires-Infection-From-Whom (WAIFW) contact matrix (Eqn 2
133 in Methods). Children aged 1-4 years not only had the largest number of infections (42.8%), but
134 also appeared to cause the largest number of infections in other age groups. Tallied over the
135 entire study period (Oct 2018-July 2019), an estimated 51.6% (95% CI: 39.3, 63.1%) of the total
136 cases were infected by 1-4 year-olds, compared to 25.2% (95% CI: 15.8, 35.5%) by 5-17 year-
137 olds, 17.7% (95% CI: 10.4, 26.5%) by 18-49 year-olds, 4.5% (95% CI: 3.0, 6.4%) by <1 year-

138 olds, and 1.0% (95% CI: 0.4, 1.8%) by 50+ year-olds. In particular, this age group caused
139 around half of the infections in infants (44.6% or 45 cases) as well as the largest proportions of
140 inter-group transmission to other age-groups (ranging from 12.9% to 5-17 year-olds to 40.1% to
141 50+ year-olds; Table 1).
142
143 *Estimated impact of vaccination campaigns*
144 Figure 5 shows the estimated outbreak outcomes had there be no vaccination campaigns.
145 Without the vaccination campaigns, the model estimated that the outbreak could continue to the
146 end of 2019 and infect a total of 6196 (95% CI: 5, 8478) people by then or 6078 (95% CI: 5,
147 8433) during the observed outbreak period (i.e. Oct 2018 – July 2019), compared to 642 cases
148 reported as of Aug 6, 2019. In addition, these infections would largely occur in infants under 1
149 and young children aged 1-4 years. During the observed outbreak period, there would be 1015
150 (95%: 0, 1430) infections in infants and 3052 (95% CI: 2, 4096) infections in 1-4 year-olds,
151 more than 10 times of the reported numbers in these two age groups (i.e. 100 and 275,
152 respectively, as of Aug 6, 2019; Table 2). Children aged 5-17 years would have the third largest
153 number of infections, with 1107 (95% CI: 1, 1692) cases, 8 times of the reported number (i.e.
154 138 as of Aug 6, 2019).
155
156 Measles can cause severe diseases. According to data by Apr 24, 2019, among 390
157 individuals with measles, 29 were hospitalized, of which six needed intensive care (*8*). Assuming
158 the same ratios among all cases, without the vaccination campaigns, during the observed
159 outbreak period there would be 452 (95% CI: 0, 628) hospitalizations, including 94 (95% CI: 0,
160 130) needing intensive care, and the majority would be in young children under 4 (Table 2).

161

162 **Discussion**

163 Using a model-filter inference system, we have reconstructed in detail the transmission dynamics
164 of the measles outbreak in an Orthodox Jewish community in NYC during Oct 2018 – July 2019.
165 We have estimated the population characteristics (e.g. age-specific susceptibilities) and
166 epidemiological parameters (e.g. reproductive numbers) as well as subtle changes in key
167 parameters (e.g. contact rates) that are critical to the transmission of measles. Using model
168 simulation and the posterior estimates from the model-inference system, we are also able to
169 estimate the impact of vaccination campaigns implemented during the outbreak, including
170 numbers of infections and hospitalizations averted, for each age group. These latter findings echo
171 those from previous studies (*9-11*) and again highlight the severity of measles disease, should
172 there be no effective infection and transmission controls (in particular, vaccination).

173

174 Our analyses estimate that around a quarter of young children aged 1-4 in the affected
175 community were susceptible at the onset of the outbreak, likely due to delayed vaccination.
176 Indeed, 94% (101/108) of the early infections in children were unvaccinated (*12*). In contrast,
177 vaccination rate remained high in older children 5-17 years, with an estimated 94% immune to
178 measles. This difference may be due to better compliance with vaccination regulation at school
179 entry, or a result of vaccination campaigns in response to previous outbreaks (e.g., a large
180 outbreak occurred in the same community in 2013 (*13*)). Nevertheless, the large number of
181 unvaccinated children under 4 was sufficient to cause many infections in late 2018,
182 predominantly in the same age group (Fig. 1 and references (*2, 12, 14*)). This observation
183 highlights the importance of vaccination compliance with both MMR vaccine doses, especially

184 given the long lag between the two vaccine doses. In addition, recommending the second MMR
185 dose earlier than the currently scheduled age 4-6 years could allow pro-vaccine parents to fully
186 vaccinate their children sooner and reduce the number of susceptible children overall.
187
188 Our study also reveals intricate interplays of population dynamics and measles
189 transmission. While the high susceptibility in children under 4 was likely responsible for the
190 early spread of measles, our estimates suggest that the second and more severe part of the
191 outbreak in 2019 was likely due to increased infectious contact among this age group, likely
192 facilitated by parents hosting "measles parties" that intentionally bring unvaccinated children
193 together and expose them to those sick with measles (*7*). As shown in Fig. 4, the increase in
194 infectious contact interacting with the high susceptibility in 1-4 year-olds was able to raise the
195 effective reproductive number R_e to above unity—the threshold for an epidemic to occur—and
196 aggravate the outbreak in 2019, despite earlier public health efforts that had reduced R_e to below
197 1 in late 2018. Similar disease-related gatherings have been noted in previous measles outbreaks
198 (*15*) as well as other disease outbreaks (*16*). These activities create further challenges for the
199 control of measles spread and stress the need for enhanced public health education.
200
201 In addition, the intensified measles outbreak not only affected children with delayed
202 vaccination, but also a large number of infants under 1, who were too young to receive their first
203 dose of MMR vaccine in the US. At least 100 infants under 1 were infected with measles during
204 the 10-month outbreak period, despite extensive infection and transmission control efforts
205 including vaccinating infants 6 months or older and post-exposure prophylaxis with immune
206 globulin given to those under 6 months (*2, 14*). This was largely a result of the high

207 susceptibility in infants. Our model-inference system estimates that about half of infants were
208 susceptible by age 1 and that nearly half of the 100 infant cases were infected by 1-4 year-olds
209 (Table 1). In addition, our simulations suggest that, without the vaccination campaigns, the
210 number of infections in infants would be over 10 times higher than observed (Table 2). These
211 findings demonstrate the rippling effects of vaccine hesitancy beyond the risk posted to age-
212 eligible children with delayed vaccination. These findings also suggest that administration of the
213 first dose of routine MMR vaccine earlier than the current 1 year age-limit in the US may be
214 necessary to protect infants should high level of vaccine hesitancy persist. Of note, the World
215 Health Organization (WHO) recommends administering the first dose of measles vaccine at 9-12
216 months of age for routine vaccination programs and as early as 6 months for settings such as
217 during an outbreak (*17*).
218
219 Our model simulations, consistent with many previous studies (*11, 15, 18*), demonstrate
220 the significant public health impact of vaccination in controlling measles outbreaks. Without the
221 implemented vaccination campaigns, the severity of the measles outbreak—including number of
222 infections, hospitalizations, and severe infections needing intensive care—would be about 10
223 times worse than observed (Table 2). These estimates, however, did not include the long-term
224 health impacts on affected individuals, particularly young children (*10, 19, 20*), nor the
225 enormous economic burdens (*13, 21, 22*).
226
227 We note several limitations of our study. First, we did not explicitly model the impact
228 of public health interventions other than the vaccination campaigns, due to a lack of data. During
229 the outbreak, such efforts included prescreening patients prior to presence for treatment, post-

230 exposure prophylaxis, and closing schools out of vaccination compliance (*2, 12, 14, 23, 24*). Of
231 note, however, here the estimated basic reproductive number R_0 was around 7, lower than the 12-
232 18 range based on epidemics in the pre-vaccine era (*25*); and the estimated infectious period was
233 around 4 days (Fig. 4C), at the lower end of the commonly used range of 4-6 days (*26*). The
234 lower R_0 and shorter infectious period could be a result of the aforementioned public health
235 interventions. Second, there were uncertainties in the accuracy of case reporting. Because the
236 incidence data used here were published on Aug 6, 2016, a later revision of case reports, we used
237 a relatively high but broad prior range for the reporting rate (i.e. 80-100%). In addition, our
238 model-inference system explicitly accounted for observational errors (Eqn 7a and 7b). Third,
239 due to a lack of contact data and for simplicity, we set all terms related to group-1 (i.e. <1 year-
240 olds) in the WAIFW matrix to the same as the contact rate within the group (Eqn 2). The model
241 formulation may have led to under-estimation of the proportions of infection in <1 year-olds
242 attributable to the same age group and/or 1-4 year-olds, given the likely more frequent contact
243 within the same age group and with similar ages (i.e. 1-4 years) due to more shared settings such
244 as daycares and pediatric hospitals. Lastly, there were uncertainties regarding the settings of
245 vaccination campaigns. Nevertheless, sensitivity analysis showed that our main estimates were
246 robust to a wide range of assumptions (Table S2).
247
248 In summary, using a comprehensive model-inference system, we have reconstructed
249 transmission dynamics of the recent measles outbreak in NYC in great detail. Our estimates
250 highlight the importance of vaccination in protecting children as well as public health education
251 to reduce activities that unnecessarily expose children to risk of measles infection. Further, in

252 light of the persistent vaccine hesitancy, revising current vaccination recommendations may
253 allow pro-vaccine parents to vaccinate and protect their children more effectively.
254

255 **Materials and Methods**

256 The measles outbreak occurred predominantly among members of the Orthodox Jewish
257 community in Williamsburg and Borough Park, two neighborhoods in located in Brooklyn,
258 NYC. As such, we focused on modeling the outbreak in this subpopulation. Estimated based on
259 the Jewish Community Study of New York (*27*), approximately *N*=165,970 Orthodox Jews live
260 in these two NYC neighborhoods, of which 4552 (2.7%), 18,208 (11%), 59,176 (35.7%), 60,445
261 (36.4%), and 23,589 (14.2%) are <1, 1-4, 5-17, 18-49, and 50+ years, respectively.
262

263 *Estimating monthly incidence by age group*

264 Monthly measles incidence aggregated over all ages from Sep 2018 to Aug 2019 and the age
265 distribution of case-patients over the entire outbreak were published on the NYC DOHMH
266 website (*3*). Of note, 1 case was reported in Sep 2018 (i.e., the initial case) and none were
267 reported in Aug 2019 at the time of this writing. In addition, the numbers of reported cases were
268 subsequently revised by the DOHMH (often adjusted upwards, presumably from retrospective
269 case identification) and, as such, varied over time. To estimate the monthly incidence for each
270 age group, we used the age distribution of cases reported in earlier health reports/alerts (*5*) to
271 apportion the total incidence for each month. For months without age information, we used
272 estimates either from the preceding month or the following month back-calculated from the
273 overall age distribution.
274

Transmission model

The transmission model used here was similar to described in our previous study (*28*). As illustrated in Fig. S1, the model represents the susceptible-exposed-infectious-recovered (SEIR) disease dynamics with five age groups (i.e. <1, 1-4, 5-17, 18-49, and 50+ years) to account for population differences by age group (e.g., susceptibility and contact rate), routine two-dose vaccination at ages 1 and 5, and immunization during the vaccination campaigns per Eqn 1:

$$\begin{cases} \frac{dS_i}{dt} = -\left(\frac{S_i^{m_1}}{N_i}\right)\sum_{j=1}^{5}\beta_{ij}\, I_j^{m_2} + k(1-v)N\mathbf{1}_{\boldsymbol{i=1}} + \frac{M}{180}\mathbf{1}_{\boldsymbol{i=1}} + l_{i-1}S_{i-1}(1-v_{i-1}) - l_iS_i - V_i(t) \\ \frac{dE_i}{dt} = \left(\frac{S_i^{m_1}}{N_i}\right)\sum_{j=1}^{5}\beta_{ij}\, I_j^{m_2} - \frac{E_i}{Z} + \alpha_i(t) + l_{i-1}E_{i-1} - l_iE_i \\ \frac{dI_i}{dt} = \frac{E_i}{Z} - \frac{I_i}{D} + l_{i-1}I_{i-1} - l_iI_i \\ \frac{dR_i}{dt} = \frac{I_i}{D} + l_{i-1}R_{i-1} - l_iR_i + l_{i-1}S_{i-1}v_{i-1} + V_i(t) \\ \frac{dM}{dt} = kvN - \frac{M}{180} \end{cases}$$

for i=1,..,5 (Eqn 1)

where S_i, E_i, I_i, R_i and N_i are, respectively, the numbers of susceptible, exposed (i.e. latently infected), infectious, recovered (and/or immunized) people and population size in the i-th age group; M is the number of infants with maternal immunity, which decays exponentially with a mean duration of 180 days; t is time in days. $V_i(t)$ is the number of people in group-i immunized by the vaccination campaigns on day-t (described in detail in the next section). The exponents m_1 and m_2 describe the level of inhomogeneous mixing (*29, 30*); and m_1=m_2=1 represents homogeneous mixing. Z and D are the latent and infectious period, respectively.

To model the different contact rates within and between age groups, we used 7 parameters for the Who-Acquires-Infection-From-Whom (WAIFW) matrix as follows:

$$\boldsymbol{\beta} = \begin{bmatrix} \beta_1 & \beta_1 & \beta_1 & \beta_1 & \beta_1 \\ \beta_1 & \beta_2 & \beta_6 & \beta_7 & \beta_1 \\ \beta_1 & \beta_6 & \beta_3 & \beta_7 & \beta_1 \\ \beta_1 & \beta_7 & \beta_7 & \beta_4 & \beta_1 \\ \beta_1 & \beta_1 & \beta_1 & \beta_1 & \beta_5 \end{bmatrix} \quad \text{(Eqn 2)}$$

where β_1 *to* β_5 represent within-group contact for the five age groups and β_6 and β_7 represent mixing between siblings and child-parent, respectively. For simplicity, we set all interactions with group 1 (i.e. <1 year) or group 5 (50+ years) to β_1, the lowest contact rate. For group-3 (5-17 years), to capture the varying contact rate following school schedules, we adjusted β_3 for each date per the school calendar in NYC as:

$$\beta_3(t) = \frac{\beta_3}{b_{Term}} \cdot [1 + b_1 Term(t)] \qquad \text{(Eqn 3)}$$

where b_1 is the amplitude of school term-time forcing; $Term(t)$ is set to 1 for school days and -1 for non-school days; and b_{Term} is the yearly average of $1+b_1 Term(t)$ (*31*).

The basic reproductive number R_0, defined as the average number of secondary infections caused by a primary case-patient in a *naïve* population, reflects the transmissibility of an infection. In an age-structured model, R_0 is computed as:

$$R_0 = \text{eigen}_{\max}(\boldsymbol{n\beta} D) \qquad \text{(Eqn 4)}$$

where $\text{eigen}_{\max}(\cdot)$ denotes the function giving the largest eigenvalue of a matrix, and $\boldsymbol{n}$ is a diagonal matrix with elements $n_i = N_i / \sum N_i$ (i=1, …, 5 here), i.e. the fraction of population in group-i. Based on this relationship between R_0 and the $\boldsymbol{\beta}$ matrix, we reparametrized the model to include R_0 as a model parameter by setting β_1 to 1 and estimating the relative magnitude of β_2–β_6, all scaled to R_0. In the current mass vaccination era, most people are immune via vaccination. To reflect the potential of an infection to cause an epidemic in a partially susceptible population, the effective reproductive number, R_e, accounts for population susceptibility and is computed as:

$$R_e = \text{eigen}_{\max}(\boldsymbol{s\beta}D) \qquad \text{(Eqn 5)}$$

where $\boldsymbol{s}$ is a diagonal matrix with elements $s_i = S_i/N_i$ (i=1, …, 5 here), i.e. the susceptibility in group-i.

To model the demographic processes, k is the birth rate (2.7 per 1000 person-year here (*27*)); v is the immunity level in mothers, approximated by the susceptibility of the child-bearing age-group (i.e., 18-49 year-olds); N is total population size; and $\mathbf{1}_{i=1}$ is an indicator function, with value 1 for group-1 (<1 year-olds) and 0 for all other groups. Thus, the term $k(1-v)\,\mathbf{1}_{i=1}$ (1st line in Eqn 1) is the number of susceptible newborns and kvN (last line in Eqn 1) is the number of newborns with maternal immunity. The term l_i is the rate of aging for group-i (i.e. the inverse of the sojourn time in each age group) with l_0 set to 0 and l_5 set to the death rate. The term v_i (for i=1 and 2) is the vaccination rate for the two doses of vaccine (i.e., v_i=0 for i=0, 3, and 4). In this study, we set v_1 (1st dose) to 0.9 times the immunity level of group-2 (i.e., assuming a 90% vaccine efficacy) and v_2 (2nd dose) to 0.7 for days before May 2019; for days afterwards, we used 0.8 for v_1 and 0.9 for v_2, corresponding to a 1-(1-0.8)(1-0.9)=98% overall vaccination rate.

Based on NYC health reports/alerts (*2, 12, 14*), we seeded the model, via the parameter $\alpha_i(t)$, with 3 cases in group-2 (i.e. 1-4 year-olds)—one each with rash onset on Sep 30, Oct 15, and Oct 30, 2018, respectively—and 1 case each in group-3 (5-17 year-olds) and group-4 (18-49 year-olds), both during the winter recess (from 12/24/18 to 1/1/19).

Modeling the vaccination campaigns

336 To contain the outbreak, the NYC DOHMH conducted extensive vaccination campaigns and
337 administered 31,790 doses of MMR vaccine to children under 19 years in Williamsburg and
338 Borough Park by July 2019 (*3*). However, information on the age and immune status of
339 vaccinees was not reported. In this study, per the health reports/alters (*3, 12*), we assumed there
340 were two phases of vaccination campaign: 1) Oct 2018 – Feb 2019, during which 7000 children,
341 90% Orthodox Jewish (15% were <1 year, 65% 1-4 years, and 20% 5-17 years) were vaccinated;
342 and 2) Mar – July 2019, during which 24,790 children, 60% Orthodox Jewish (10%, 40%, and
343 50%, respectively, were <1, 1-4, and 5-17 years) were vaccinated. For reference, Orthodox Jews
344 made up for approximately 30% of the total population in the two affected neighborhoods.
345
346 For <1 year-olds, immunization could fail due to residual maternal immunity; thus, we
347 assumed a 85% immunization success rate for group-1. For those above 1 year, some vaccinees
348 might have received 1 or 2 doses of vaccine and higher the population susceptibility, the less
349 likely a vaccinee had been immune before the additional vaccine dose. As such, we assumed the
350 immunization success rate was twice the group-specific susceptibility for 1-4 year-olds and three
351 times that for 5-17 year-olds or at a minimum of 25% and a maximum of 75%. We further
352 assumed a 10-day delay in vaccine effect and computed the daily number of individuals
353 vaccinated per a gamma distribution (mean=30 days and standard deviation=21 days for Phase-1
354 and mean=56 and standard deviation=15 days for Phase-2 such that it peaked ~1 week after Apr
355 9, 2019 when the city implemented a vaccination mandate). The estimated numbers matched
356 with the reports (e.g., 1740 doses by our model vs ~1600 doses given to children under 5 as
357 reported (*32*) and 1142 doses by our model vs ~1000 doses given in March 2019 as reported (*7,*

358 *33*)). These daily numbers were then included in the transmission model [i.e. $V_i(t)$ in Eqn 1].
359 Sensitivity to model assumptions were tested as described below.
360
361 *Estimation of model state variables and parameters*
362 To estimate the model state variables (i.e., S_i, E_i, I_i, R_i, and M) and parameters (β_2 *to* β_7, R_0, b_1, D,
363 Z, m_1, *and* m_2), we fitted the model to the reported monthly overall incidence and the estimated
364 monthly age-grouped incidence using a particle filter (*34*). Briefly, we first initialized a suite of
365 model realizations (termed "particles", N=10,000 here) using Latin Hypercube sampling (*35*)
366 from the prior distribution of state variables and parameters (Table S1). The particle filter then
367 sequentially incorporated the monthly incidence to the model via repeated prediction-update
368 cycles. In each cycle (i.e., each month here), the particles were stochastically integrated forward
369 in time for a month per the model (i.e., Eqn 1; this generates the prediction). To update the model
370 state including all model variables and parameters, at the end of each month, the model-
371 estimated incidence was aggregated for the month, adjusted by the reporting rate for that month
372 (estimated simultaneously by the filter), and used to compute the likelihood of each particle
373 (described below). The posterior of model state was then computed using Bayes' rule (*34, 36*)
374 and the particles resampled and updated—those with high posterior probabilities were retained
375 and those with very low posterior probabilities discarded.
376
377 To allow for a wider observational variance than, e.g., the Poisson process, we
378 heuristically modeled the observations using a multivariate Gaussian distribution (i.e. the
379 likelihood function):
380 $$\boldsymbol{Y_m} | r, \boldsymbol{C_m} \sim \mathcal{N}(r\boldsymbol{C_m}, \boldsymbol{\Sigma}) \quad \text{(Eqn 6)}$$

where $\boldsymbol{Y_m}$ is the vector of monthly incidence reported for month-m, including the monthly incidence for individual age-groups (i.e., <1, 1-4, 5-17 and 18+ years; note that 18-49 and 50+ year-olds were combined due to a lack of data for these two groups separately) and all ages combined. Correspondingly, $\boldsymbol{C_m}$ is the vector of monthly incidence estimated by the model; and r is the reporting rate and, for simplicity, assumed the same for all ages. $\boldsymbol{\Sigma}$ is the covariance matrix, with the off-diagonal terms set to 0. To account for uncertainties in the estimated age-grouped incidence, the variance ($\Sigma_{ii}, i = 1, \ldots, 4$) for each of the 4 aforementioned age-groups was heuristically computed as:

$$\Sigma_{ii,m} = 100 + \frac{\left(\sum_{m}^{m-2} Y_m/3\right)^2}{3} \quad \text{(Eqn 7a)}$$

That is, the observational variance is proportional to the average incidence in the preceding two months (if available) and the current month, plus a baseline constant. For the overall incidence with detailed data, a smaller variance was used:

$$\Sigma_{ii,m} = 100 + \frac{\left(\sum_{m}^{m-2} Y_m/3\right)^2}{5} \quad \text{(Eqn 7b)}$$

As there were great uncertainties in the susceptibilities of the younger age groups, we tested prior ranges from 10-40% for 1-4 year-olds, 5-20% for 5-17 year-olds, and 5-15% for 18-49 year-olds. For the basic reproductive number R_0, we tested prior values ranging from 5 to 12 (note these values were lower than the oft-reported 12-18 range (*6, 25*)). To optimize the model-filter system, we parsed these wide ranges into smaller segments and tested all combinations by permutation (5040 in total; see specific prior ranges in Table S1). To account for model stochasticity, we ran the model-filter system 5 times for each prior combination and 10 times for the final prior select. We then selected the optimal priors based on the model-goodness-of-fit to

404 the data (minimal root-mean-square-error and maximal correlation and likelihood) over the
405 period of Oct 2018 – July 2019 as well as accuracy of the one-step-ahead predictions (recall that
406 the particle filtering process comprises sequential prediction-update cycles) for the period of Oct
407 2018 – March 2019 (i.e. before the emergency vaccination mandate). We pooled all 10 final runs
408 (10,000 particles each run and 100,000 model realizations in total) to compute the posterior
409 estimates (e.g., mean and 95% CI).
410
411 *Sensitivity analysis on vaccination campaigns settings*
412 To test the sensitivity of model results to assumptions on vaccination campaign settings, we
413 tested the model-filter system using the following alternative scenarios:
414 1) For the 2nd phase (Mar-July 2019), 90% (vs. 60% in the baseline scenario) of the
415 vaccine doses were given to members of the Orthodox Jewish community;
416 2) For the 2nd phase, the age distribution of vaccinees was the same as the 1st phase (i.e.
417 15%, 65%, and 20%, respectively, for <1, 1-4, and 5-17 year-olds vs. 10%, 40%, and 50% for
418 the three groups in the baseline scenario);
419 3) For the 2nd phase, 90% of the vaccine doses were given to Orthodox Jewish and the
420 age distribution of vaccinees was the same as the 1st phase (i.e. 15%, 65%, and 20% for <1, 1-4,
421 and 5-17 year-olds, respectively).
422
423 Because population susceptibility would be affected by the number of individuals
424 immunized by the vaccination campaigns, we tested susceptibility ranges 10-40% for 1-4 year-
425 olds, 5-20% for 5-17 year-olds, and 5-15% for 18-49 year-olds, divided in to small segments as
426 for the baseline scenario (140 different combinations for each alternative scenario; Table S1).

427 For simplicity, we used the same optimal prior ranges for the parameters under the baseline
428 scenario in this sensitivity analysis.
429
430 ***Evaluating the impact of vaccination campaigns***
431 To estimate the impact of vaccination campaigns, we generated model-simulated
432 counterfactuals—i.e., outbreak outcomes should there be no vaccination campaigns
433 implemented—using the posterior mean estimates of group-specific initial population
434 susceptibilities and model parameters for each month. We ran the model (10,000 realizations)
435 stochastically up to the end of 2019 to test how long the outbreak could last without intervention;
436 for months after Aug 2019, parameters estimated at the end of July 2019 were used.
437
438 **Acknowledgements**
439 This study was supported by the National Institute of Allergy and Infectious Diseases
440 (1R01AI145883-01). I thank all public health personnel and individuals involved in combating
441 the measles outbreak and New York City Department of Health and Mental Hygiene for making
442 the incidence data publicly available. I also thank Columbia University Mailman School of
443 Public Health for access to high performance computing.
444 **Conflict of interest:** None.
445
446 **References:**
447 1. V. K. Phadke, R. A. Bednarczyk, D. A. Salmon, S. B. Omer, Association Between Vaccine
448 Refusal and Vaccine-Preventable Diseases in the United States A Review of Measles and
449 Pertussis. *Jama-J Am Med Assoc* **315**, 1149-1158 (2016).

450 2. New York City Department of Health and Mental Hygiene, ALERT # 39: Update on
451 Measles Outbreak in New York City in the Orthodox Jewish Community. (2018).
452 https://www1.nyc.gov/assets/doh/downloads/pdf/han/alert/2018/alert39-measles-
453 outbreak.pdf.
454 3. New York City Department of Health and Mental Hygiene, Measles. (2019).
455 https://www1.nyc.gov/site/doh/health/health-topics/measles.page.
456 4. New York City Department of Health and Mental Hygiene, Order of the Commissioner.
457 (2019). 4/9/19. https://www1.nyc.gov/assets/doh/downloads/pdf/press/2019/emergency-
458 orders-measles.pdf.
459 5. New York City Department of Health and Mental Hygiene, Health Alert Network. (2019).
460 https://www1.nyc.gov/site/doh/providers/resources/health-alert-network.page.
461 6. F. M. Guerra, S. Bolotin, G. Lim, J. Heffernan, S. L. Deeks, Y. Li, N. S. Crowcroft, The
462 basic reproduction number (R0) of measles: a systematic review. *Lancet Infect Dis* **17**, e420-
463 e428 (2017).
464 7. S. Scutti, New York City declares a public health emergency amid Brooklyn measles
465 outbreak. (2019). 4/9/19. https://www.cnn.com/2019/04/09/health/measles-new-york-
466 emergency-bn/index.html.
467 8. New York City Department of Health and Mental Hygiene, ALERT # 9: Citywide
468 Recommendations during the Ongoing Measles Outbreak in New York City. (2019).
469 https://www1.nyc.gov/assets/doh/downloads/pdf/han/alert/2019/recommendations-during-
470 measles-outbreak.pdf.

471 9. M. J. Mina, B. T. Grenfell, C. J. E. Metcalf, Response to Comment on "Long-term measles-
472 induced immunomodulation increases overall childhood infectious disease mortality".
473 *Science* **365**, (2019).
474 10. M. J. Mina, C. J. E. Metcalf, R. L. de Swart, A. D. M. E. Osterhaus, B. T. Grenfell, Long-
475 term measles-induced immunomodulation increases overall childhood infectious disease
476 mortality. *Science* **348**, 694-699 (2015).
477 11. P. A. Gastanaduy, S. Funk, P. Paul, L. Tatham, N. Fisher, J. Budd, B. Fowler, S. de Fijter,
478 M. DiOrio, G. S. Wallace, B. Grenfell, Impact of Public Health Responses During a Measles
479 Outbreak in an Amish Community in Ohio: Modeling the Dynamics of Transmission. *Am J*
480 *Epidemiol* **187**, 2002-2010 (2018).
481 12. New York City Department of Health and Mental Hygiene, ALERT # 2: Update on Measles
482 Outbreak in New York City in the Orthodox Jewish Community. (2019).
483 https://www1.nyc.gov/assets/doh/downloads/pdf/han/alert/2019/update-on-measles-
484 outbreak-in-nyc-in-the-orthodox-jewish-community.pdf.
485 13. J. B. Rosen, R. J. Arciuolo, A. M. Khawja, J. Fu, F. R. Giancotti, J. R. Zucker, Public Health
486 Consequences of a 2013 Measles Outbreak in New York City. *JAMA Pediatr* **172**, 811-817
487 (2018).
488 14. New York City Department of Health and Mental Hygiene, ALERT # 38: Measles Outbreak
489 in New York City in the Orthodox Jewish Community. (2018).
490 https://www1.nyc.gov/assets/doh/downloads/pdf/han/alert/2018/alert38-measles-
491 outbreak.pdf.
492 15. P. A. Gastanaduy, E. Banerjee, C. DeBolt, P. Bravo-Alcantara, S. A. Samad, D. Pastor, P. A.
493 Rota, M. Patel, N. S. Crowcroft, D. N. Durrheim, Public health responses during measles

494 outbreaks in elimination settings: Strategies and challenges. *Human vaccines &*
495 *immunotherapeutics* **14**, 2222-2238 (2018).
496 16. Centers for Disease Control and Prevention, Chickenpox (Varicella): Transmssion. (2018).
497 December 31, 2018. https://www.cdc.gov/chickenpox/about/transmission.html.
498 17. W. H. Organization, Measles vaccines: WHO position paper, April 2017–
499 Recommendations. *Vaccine*, (2017).
500 18. J. Lessler, C. J. E. Metcalf, F. T. Cutts, B. T. Grenfell, Impact on Epidemic Measles of
501 Vaccination Campaigns Triggered by Disease Outbreaks or Serosurveys: A Modeling Study.
502 *Plos Medicine* **13**, (2016).
503 19. P. E. Christensen, H. Schmidt, H. O. Bang, V. Andersen, B. Jordal, O. Jensen, An epidemic
504 of measles in southern Greenland, 1951; measles in virgin soil. III. Measles and tuberculosis.
505 *Acta Med Scand* **144**, 450-454 (1953).
506 20. P. E. Christensen, H. Schmidt, H. O. Bang, V. Andersen, B. Jordal, O. Jensen, An epidemic
507 of measles in southern Greenland, 1951; measles in virgin soil. II. The epidemic proper.
508 *Acta Med Scand* **144**, 430-449 (1953).
509 21. S. Y. Chen, S. Anderson, P. K. Kutty, F. Lugo, M. McDonald, P. A. Rota, I. R. Ortega-
510 Sanchez, K. Komatsu, G. L. Armstrong, R. Sunenshine, J. F. Seward, Health Care-
511 Associated Measles Outbreak in the United States After an Importation: Challenges and
512 Economic Impact. *Journal of Infectious Diseases* **203**, 1517-1525 (2011).
513 22. G. H. Dayan, I. R. Ortega-Sanchez, C. W. LeBaron, M. P. Quinlisk, I. M. R. Team, The cost
514 of containing one case of measles: The economic impact on the public health infrastructure -
515 Iowa, 2004. *Pediatrics* **116**, E1-E4 (2005).

23. T. Pager, Measles Outbreak: Yeshiva's Preschool Program Is Closed by New York City Health Officials. (2019). 4/15/2019. https://www.nytimes.com/2019/04/15/nyregion/measles-nyc-yeshiva-closing.html.

24. A. Sanders, NYC health officials close two more Williamsburg yeshivas for failure to show immunization records amid measles outbreak. (2019). 6/13/2019. https://www.nydailynews.com/news/politics/ny-city-closes-williamsburg-brooklyn-yeshivas-measles-outbreak-20190613-jogozcbe65ejtalweq255lwkka-story.html.

25. R. M. Anderson, R. M. May, *Infectious diseases of humans: dynamics and control*. (Oxford University Press, Oxford, 1991).

26. M. J. Keeling, B. T. Grenfell, Disease extinction and community size: Modeling the persistence of measles. *Science* **275**, 65-67 (1997).

27. P. Beck, S. M. Cohen, J. B. Ukeles, R. Miller, Jewish Community Study of New York: 2011, Geographic Profile. revised ed. *New York City: UJA-Federation of New York*, (2013).

28. W. Yang, J. Li, J. Shaman, Characteristics of measles epidemics in China (1951-2004) and implications for elimination: A case study of three key locations. *Plos Comput Biol* **15**, e1006806 (2019).

29. B. F. Finkenstädt, B. T. Grenfell, Time series modelling of childhood diseases: a dynamical systems approach. *Journal of the Royal Statistical Society: Series C (Applied Statistics)* **49**, 187-205 (2000).

30. W.-m. Liu, H. W. Hethcote, S. A. Levin, Dynamical behavior of epidemiological models with nonlinear incidence rates. *Journal of mathematical biology* **25**, 359-380 (1987).

31. M. J. Keeling, P. Rohani, in *Modeling Infectious Diseases in Humans and Animals*. (Princeton University Press, 2008), chap. 5, pp. 155.

32. New York City Department of Health and Mental Hygiene, Health Department Reports Eleven New Cases of Measles in Brooklyn's Orthodox Jewish Community, Urges On Time Vaccination for All Children, Especially Before Traveling to Israel and Other countries Experiencing Measles Outbreaks. (2018). https://www1.nyc.gov/site/doh/about/press/pr2018/pr091-18.page.
33. New York City Department of Health and Mental Hygiene, Measles Outbreak in Orthodox Jewish Community of Brooklyn Continues to Grow — Health Department Urges Parents to Vaccinate Their Children. (2019). 2/28/19. https://www1.nyc.gov/site/doh/about/press/pr2019/measles-outbreak-now-at-121-cases.page.
34. M. S. Arulampalam, S. Maskell, N. Gordon, T. Clapp, A tutorial on particle filters for online nonlinear/non-Gaussian Bayesian tracking. *IEEE Trans. Signal Process.* **50**, 174-188 (2002).
35. M. D. McKay, R. J. Beckman, W. J. Conover, Comparison of three methods for selecting values of input variables in the analysis of output from a computer code. *Technometrics* **21**, 239-245 (1979).
36. W. Yang, A. Karspeck, J. Shaman, Comparison of filtering methods for the modeling and retrospective forecasting of influenza epidemics. *PLoS Comput Biol* **10**, e1003583 (2014).

Figure Captions:

Fig. 1. Monthly incidence for all ages and by age group. The solid line (y-axis on the right) shows monthly incidence for all ages, reported as of Aug 6, 2019. For comparison, bars (y-axis on the left) show monthly incidence for <1 (blue), 1-4 (orange), 5-17 (grey) and 18+ (yellow) year-olds, respectively, estimated based on health reports.

Fig. 2. Model fit. Box plots show estimates of monthly incidence for all ages (A), percentage of cases reported in each age group (B), and monthly incidence for <1 year-olds (C), 1-4 year-olds (D), 5-17 year-olds (E), and 18+ year-olds (F). Results are pooled over all 10 model-filter runs (each with 10,000 and in total 100,000 model realizations). Horizontal thick lines show the median of model estimates; box edges show the 25th and 75th percentiles; whiskers show the 2.5^{th} and 97.5^{th} percentiles; and dots show outliers. Stars (*) in A and B show monthly incidence for all ages and the age distribution, reported as of Aug 6, 2019; crosses (x) in C-F show age-grouped monthly incidence estimated from health reports.

Fig. 3. Estimated changes in population susceptibility. Red lines and surrounding areas (y-axis on the left) show the mean and 95% credible intervals of estimates pooled over all 10 model-filter runs (100,000 model realizations in total) for <1 year-olds (A), 1-4 year-olds (B), 5-17 year-olds (C) and 18+ year-olds (D), respectively, at the end of each month from Sep 2018 to July 2019. The initial susceptibilities, estimated at the end of Sep 2018, were computed by adding the total numbers of individuals immunized by the vaccination campaigns in Oct 2018 to the posterior estimates at the end of Oct 2018. For comparison, the grey bars (y-axis on the right) show estimated numbers of individuals immunized during the vaccination campaigns; note that the vaccination campaigns targeted individuals under 19 years and thus is not shown for 18+ year-olds.

Fig. 4. Estimates of key model parameters: (A) the basic reproductive number, (B) the effective reproductive number, (C) infectious period, (D) relative contact rate among 1-4 year-olds, (E) relative contact rate among 5-17 year-olds, and (F) relative contact rate among 18-49 year-olds. Red lines and surrounding areas (y-axis on the left) show the mean and 95% credible intervals of estimates pooled over all 10 model-filter runs (100,000 model realizations in total) made at the end of each month from Oct 2018 to July 2019. For comparison, the grey bars (y-axis on the left) show monthly incidence for all ages (A-C) or the related age groups (D-F).

Fig. 5. Estimated impact of vaccination campaigns. Box plots show simulated estimates of monthly incidence for all ages (A), percentage of cases reported in each age group (B), and monthly incidence for <1 year-olds (C), 1-4 year-olds (D), 5-17 year-olds (E), and 18+ year-olds (F), should there be no vaccination campaigns. Results are pooled over 10,000 model simulations. Horizontal thick lines show the median of model estimates; box edges show the 25th and 75th percentiles; whiskers show the 2.5^{th} and 97.5^{th} percentiles; and dots show outliers. For comparison, stars (*) in A and B show monthly incidence for all ages and the age distribution, reported as of Aug 6, 2019; crosses (x) in C-F show age-grouped monthly incidence estimated from health reports.

Table Captions:

Table 1. Estimated proportion of infections caused by each age-group. Rows show the receiving (i.e. infectee) age groups and columns show the source of infection (i.e. infector age group). The numbers are the mean (and 95% CI) estimates in percentage. For instance, for <1 year-olds (3rd row), on average 16.3% of cases were infected by the same age group, 44.6% by 1-4 year-olds, 20.9% by 5-17 year-olds, 15.2% by 18-49 year-olds, and 3% by 50+ year-olds.

Table 2. Estimated impact of vaccination campaigns during Oct 2018 – July 2019. Columns 2-4 show the total numbers of infections (2nd column), hospitalizations (3rd column), and individuals in intensive care unit (ICU) for different age groups (rows 3 to 6) and overall (last row), should there be no vaccination campaigns. Columns 5-7 show the number of infections, hospitalizations, and ICU cases averted by the vaccination campaigns, compared to data reported as of Aug 6, 2019. Numbers are the mean (and 95% confidence intervals) of 10,000 simulations.

TABLES

Table 1. Estimated proportion of infections caused by each age-group. Rows show the receiving (i.e. infectee) age groups and columns show the source of infection (i.e. infector age group). The numbers are the mean (and 95% CI) estimates in percentage. For instance, for <1 year-olds (3rd row), on average 16.3% of cases were infected by the same age group, 44.6% by 1-4 year-olds, 20.9% by 5-17 year-olds, 15.2% by 18-49 year-olds, and 3% by 50+ year-olds.

Infectee age groups	Infector age groups				
	<1 year	1-4 years	5-17 years	18-49 years	50+ years
<1 year	16.3 (12.3, 21.0)	44.6 (35.5, 53.5)	20.9 (13.9, 28.4)	15.2 (9.6, 21.6)	3.0 (1.4, 5.0)
1-4 years	1.8 (1.0, 3.0)	85.8 (77.0, 91.9)	7 (3.2, 12.9)	5 (2.2, 9.3)	0.3 (0.1, 0.6)
5-17 years	1.5 (0.9, 2.4)	12.9 (6.9, 21.3)	80.9 (70.4, 88.4)	4.4 (2, 8)	0.3 (0.1, 0.5)
18-49 yeas	2.4 (1.5, 3.7)	18.6 (10.9, 28.0)	9.1 (4.8, 14.9)	69.5 (56.2, 80.8)	0.4 (0.2, 0.8)
50+ years	15.5 (11.6, 19.9)	40.1 (31.1, 49.3)	19.7 (13, 27)	15.6 (9.7, 22.4)	9.1 (3.8, 16.3)

Table 2. Estimated impact of vaccination campaigns during Oct 2018 – July 2019. Columns 2-4 show the total numbers of infections (2nd column), hospitalizations (3rd column), and individuals in intensive care unit (ICU) for different age groups (rows 3 to 6) and overall (last row), should there be no vaccination campaigns. Columns 5-7 show the number of infections, hospitalizations, and ICU cases averted by the vaccination campaigns, compared to data reported as of Aug 6, 2019. Numbers are the mean (and 95% confidence intervals) of 10,000 simulations.

Age group	No. if without vaccination campaigns			No. averted by vaccination campaigns		
	Infection	Hospitalization	ICU	Infections	Hospitalization	ICU
<1	1015 (0, 1430)	75 (0, 106)	16 (0, 22)	937 (0, 1330)	70 (0, 99)	14 (0, 20)
4-5	3052 (3, 4096)	227 (0, 305)	47 (0, 63)	2837 (0, 3821)	211 (0, 284)	44 (0, 59)
5-17	1107 (1, 1692)	82 (0, 126)	17 (0, 26)	999 (0, 1554)	74 (0, 116)	15 (0, 24)
18+	904 (1, 1343)	67 (0, 100)	14 (0, 21)	803 (0, 1214)	60 (0, 90)	12 (0, 19)
All	6078 (5, 8443)	452 (0, 628)	94 (0, 130)	5576 (0, 7801)	415 (0, 580)	86 (0, 120)

FIGURES

Fig. 1. Monthly incidence for all ages and by age group. The solid line (y-axis on the right) shows monthly incidence for all ages, reported as of Aug 6, 2019. For comparison, bars (y-axis on the left) show monthly incidence for <1 (blue), 1-4 (orange), 5-17 (grey) and 18+ (yellow) year-olds, respectively, estimated based on health reports.

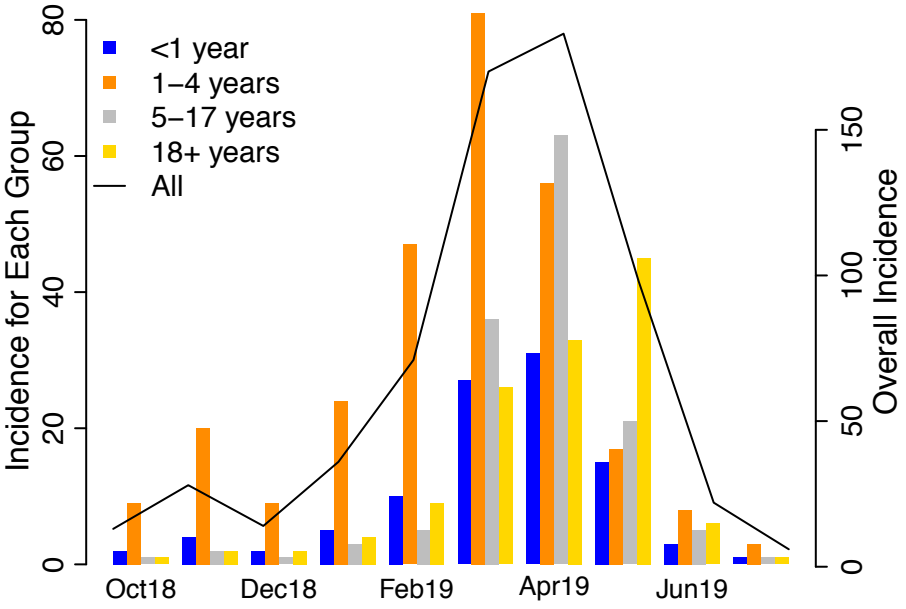

Fig. 2. Model fit. Box plots show estimates of monthly incidence for all ages (A), percentage of cases reported in each age group (B), and monthly incidence for <1 year-olds (C), 1-4 year-olds (D), 5-17 year-olds (E), and 18+ year-olds (F). Results are pooled over all 10 model-filter runs (each with 10,000 and in total 100,000 model realizations). Horizontal thick lines show the median of model estimates; box edges show the 25th and 75th percentiles; whiskers show the 2.5th and 97.5th percentiles; and dots show outliers. Stars (*) in A and B show monthly incidence for all ages and the age distribution, reported as of Aug 6, 2019; crosses (x) in C-F show age-grouped monthly incidence estimated from health reports.

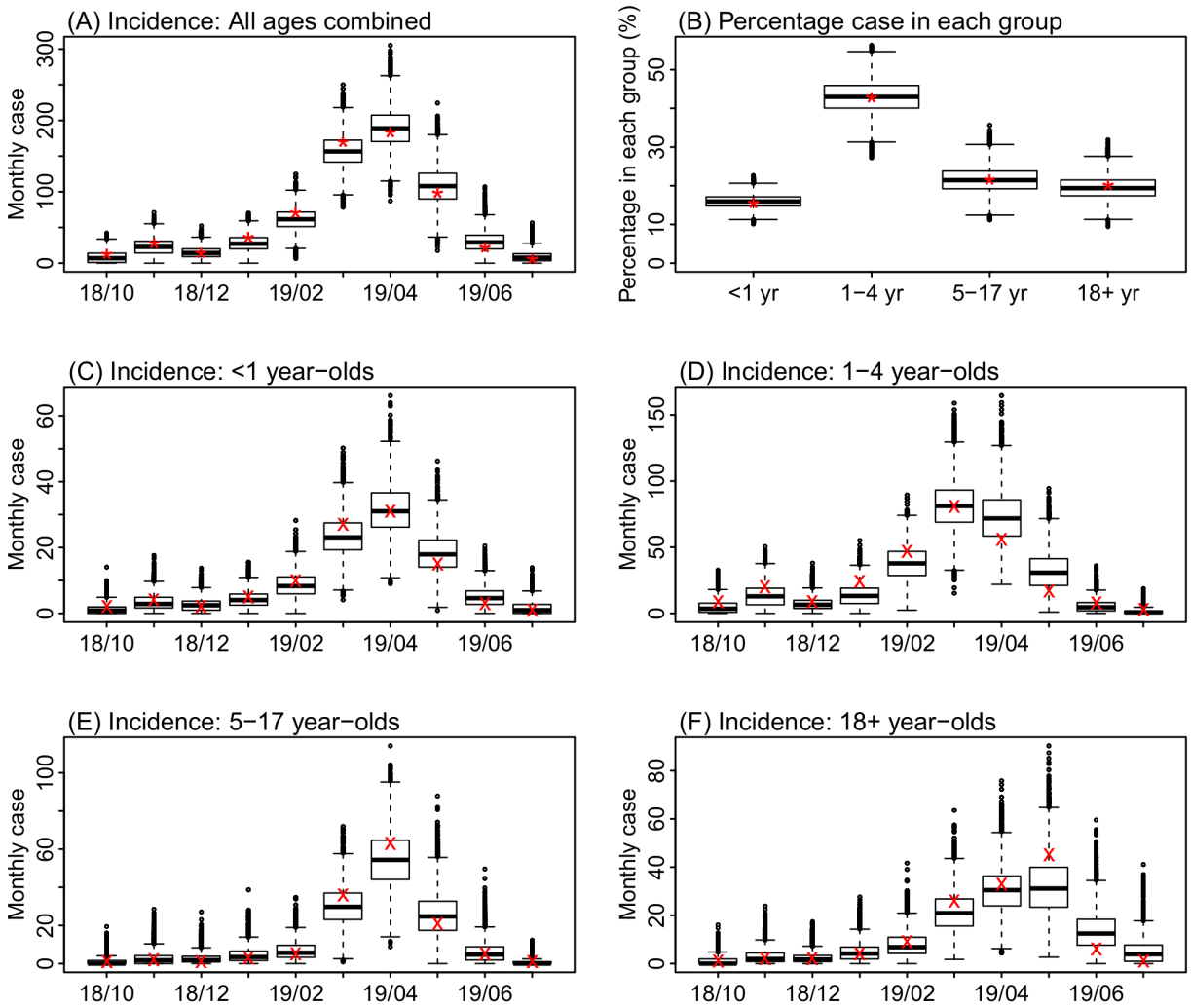

Fig. 3. Estimated changes in population susceptibility. Red lines and surrounding areas (y-axis on the left) show the mean and 95% credible intervals of estimates pooled over all 10 model-filter runs (100,000 model realizations in total) for <1 year-olds (A), 1-4 year-olds (B), 5-17 year-olds (C) and 18+ year-olds (D), respectively, at the end of each month from Sep 2018 to July 2019. The initial susceptibilities, estimated at the end of Sep 2018, were computed by adding the total numbers of individuals immunized by the vaccination campaigns in Oct 2018 to the posterior estimates at the end of Oct 2018. For comparison, the grey bars (y-axis on the right) show estimated numbers of individuals immunized during the vaccination campaigns; note that the vaccination campaigns targeted individuals under 19 years and thus is not shown for 18+ year-olds.

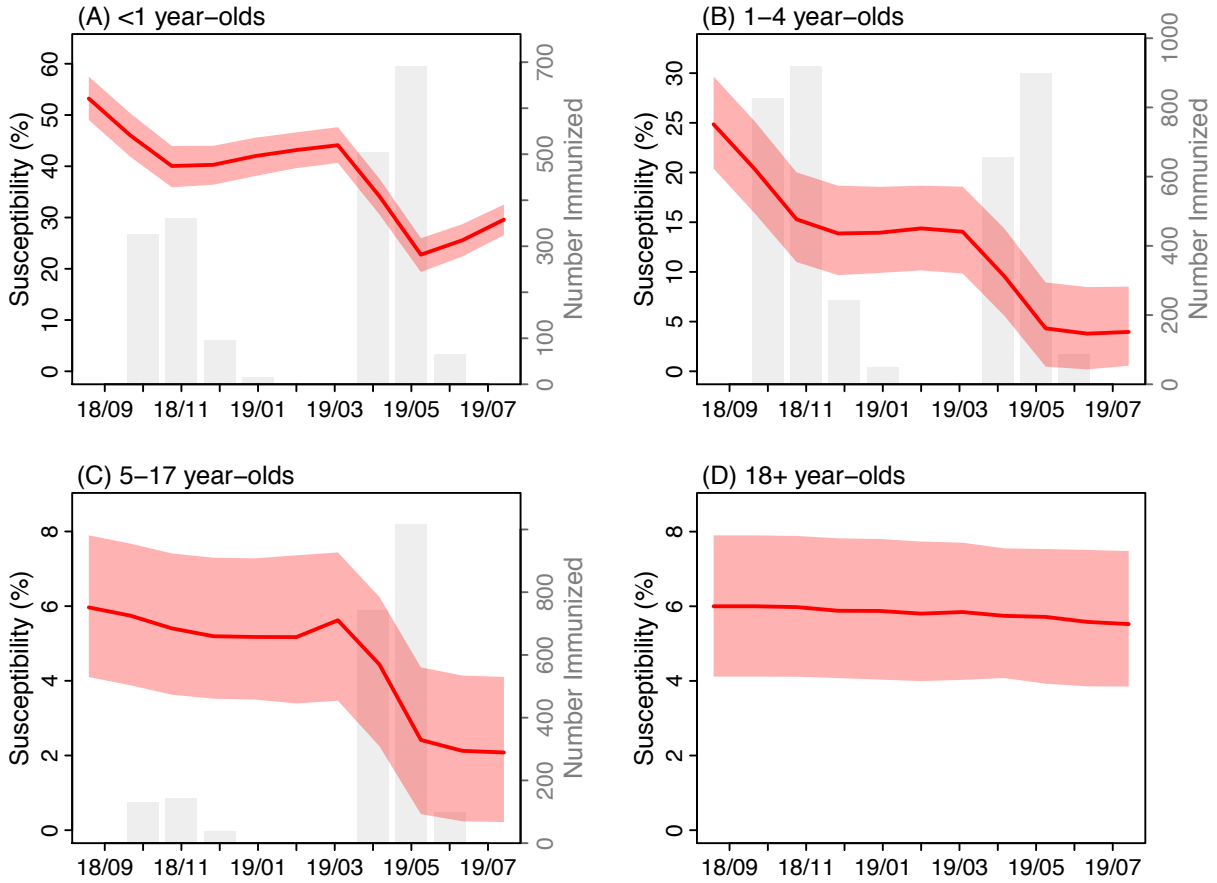

Fig. 4. Estimates of key model parameters: (A) the basic reproductive number, (B) the effective reproductive number, (C) infectious period, (D) relative contact rate among 1-4 year-olds, (E) relative contact rate among 5-17 year-olds, and (F) relative contact rate among 18-49 year-olds. Red lines and surrounding areas (y-axis on the left) show the mean and 95% credible intervals of estimates pooled over all 10 model-filter runs (100,000 model realizations in total) made at the end of each month from Oct 2018 to July 2019. For comparison, the grey bars (y-axis on the left) show monthly incidence for all ages (A-C) or the related age groups (D-F).

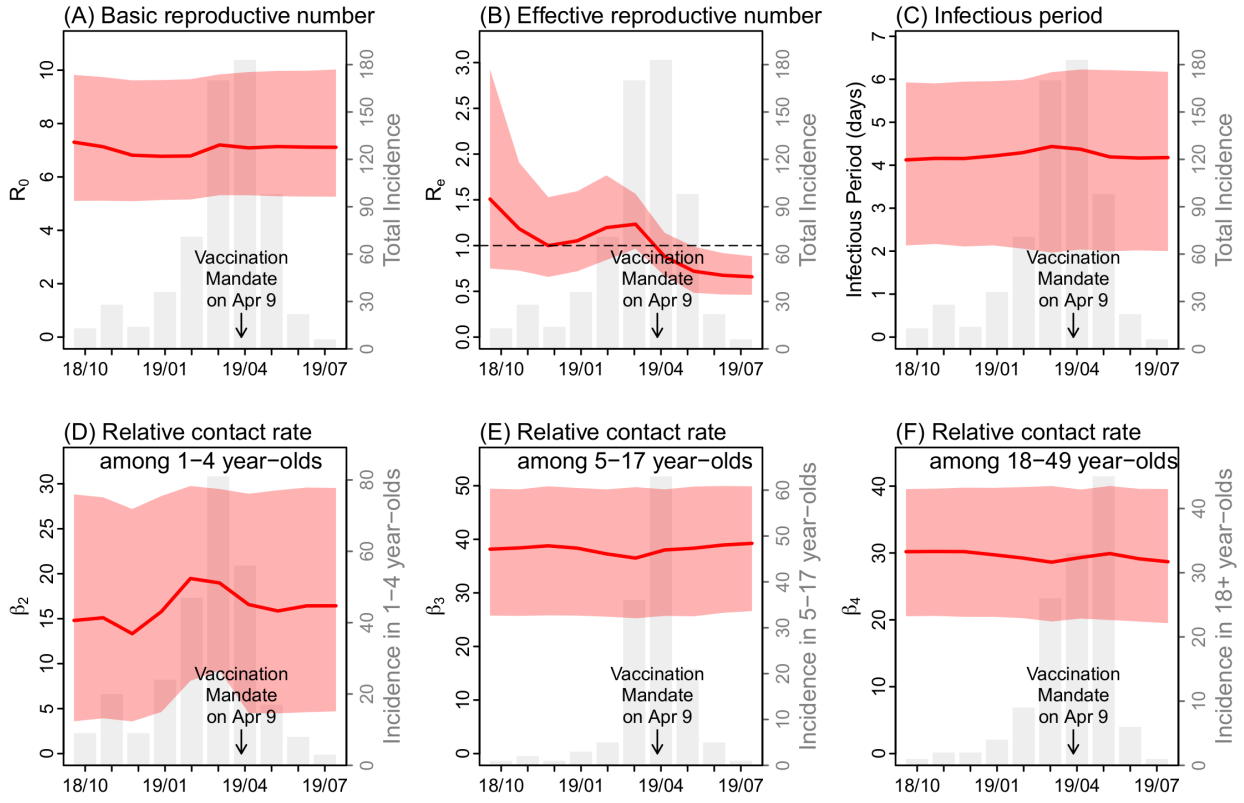

Fig. 5. Estimated impact of vaccination campaigns. Box plots show simulated estimates of monthly incidence for all ages (A), percentage of cases reported in each age group (B), and monthly incidence for <1 year-olds (C), 1-4 year-olds (D), 5-17 year-olds (E), and 18+ year-olds (F), should there be no vaccination campaigns. Results are pooled over 10,000 model simulations. Horizontal thick lines show the median of model estimates; box edges show the 25th and 75th percentiles; whiskers show the 2.5th and 97.5th percentiles; and dots show outliers. For comparison, stars (*) in A and B show monthly incidence for all ages and the age distribution, reported as of Aug 6, 2019; crosses (x) in C-F show age-grouped monthly incidence estimated from health reports.

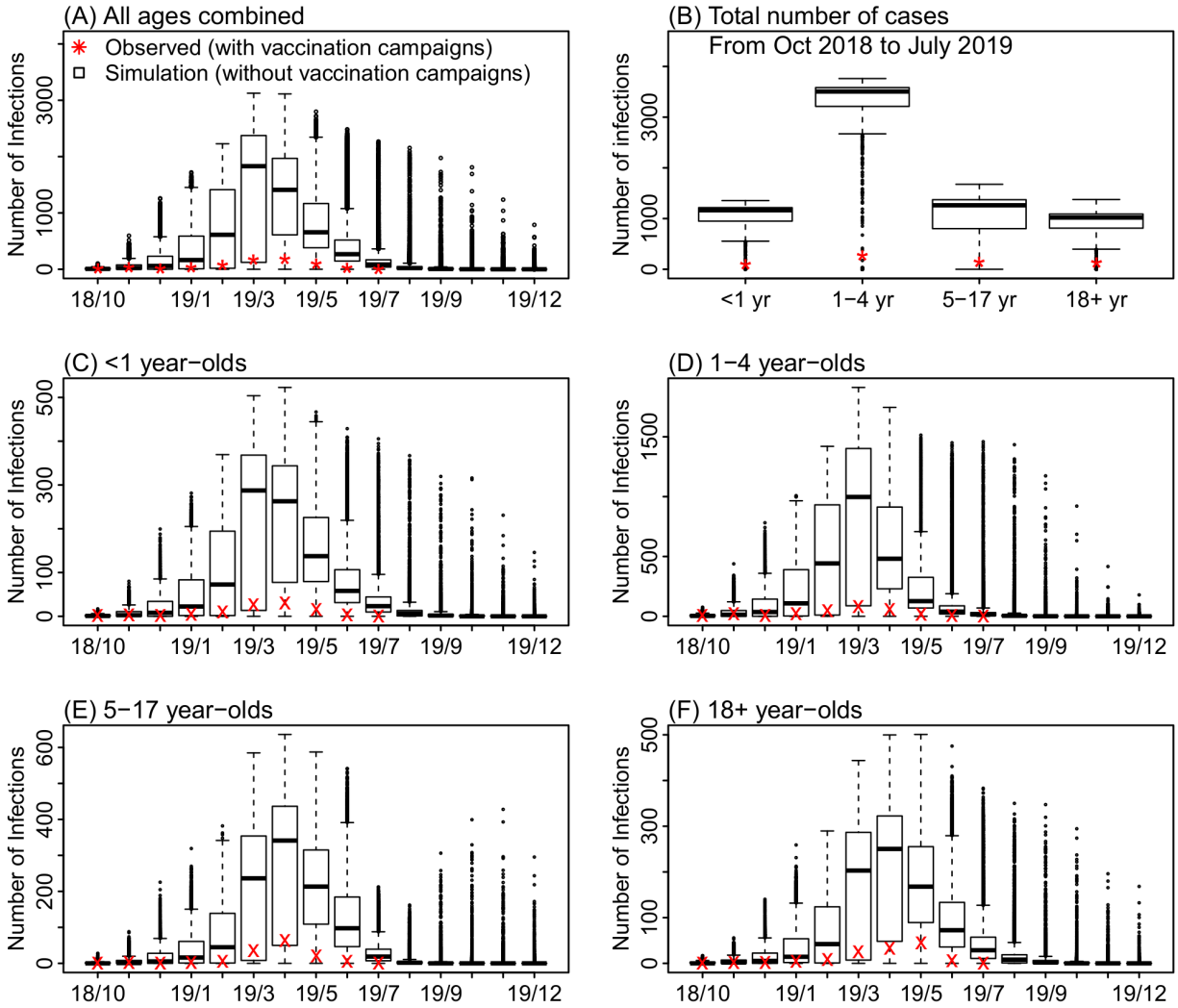

Supplementary Materials

Table S1. Main model parameters and prior ranges tested. In total, we tested 5040 combinations of prior ranges. Each combination was used as the lower and upper bounds of Latin Hypercube sampling. The optimal prior used in the final model-filter runs are bolded if multiple ranges were tested.

Parameter	Symbol/Equation	Ranges tested
Initial susceptibility in <1 year-olds	S_1(t=0); Eqn 1	Based on susceptibility in 18-49 year-olds (i.e., the mothers)
Initial susceptibility in 1-4 year-olds	S_2(t=0); Eqn 1	[5, 15], [10, 20], [15, 25], **[20, 30]**, [25, 35], [30, 40], [35, 45]%
Initial susceptibility in 5-17 year-olds	S_3(t=0); Eqn 1	**[4, 8]**, [5, 10], [5, 15], [10, 20], [15, 25]%
Initial susceptibility in 18-49 year-olds	S_4(t=0); Eqn 1	**[4, 8]**, [5, 10], [5, 15], [10, 20]%
Initial susceptibility in 50+ year-olds	S_5(t=0); Eqn 1	[4, 8]%
Initial number of infants with maternal immunity	M(t=0); Eqn 1	Based on susceptibility in 18-49 year-olds (i.e., the mothers)
Latent period	Z; Eqn 1	[7, 9] days
Infectious period	D; Eqn 1	[2, 6] days
Mixing parameter for the susceptibles	m_1; Eqn 1	**1** (perfect mixing), [0.95, 1], [0.9, 0.95]
Mixing parameter for the infectious	m_2; Eqn 1	**1** (perfect mixing), [0.95, 1], [0.9, 0.95]
Relative contact rate among <1 year-olds	β_1; Eqn 2	Set to 1
Relative contact rate among 1-4 year-olds	β_2; Eqn 2	[3, 30]
Relative contact rate among 5-17 year-olds	β_3; Eqn 2	[25, 50]
Relative contact rate among 18-49 year-olds	β_4; Eqn 2	[20, 40]
Relative contact rate among 50+ year-olds	β_5; Eqn 2	[1, 5]
Relative contact rate between 1-4 and 5-17 year-olds (sibling interactions)	β_6; Eqn 2	[1, 5]
Contact rate between 18-49 and 1-4 or 5-17 year-olds (parent-child interactions)	β_7; Eqn 2	[1, 5]
Amplitude of school term-time forcing	b_1; Eqn 3	[0.25, 0.75], **[0.5, 1]**
Basic reproductive number	R_0; Eqn 4	**[5, 10]**, [7, 12]
Reporting rate	r; Eqn 6	[80, 100]%

Table S2. Comparison of model estimates on initial susceptibility and model performance under different assumptions on vaccination campaigns. The baseline setting is as reported in the main text and alternative settings 1 to 3 are as described in the section "*Sensitivity analysis on vaccination campaigns settings.*" The results are summarized by pooling all 10 model-filter runs (10,000 particles each run and 100,000 model realizations in total). The numbers are the mean and, for the susceptibilities, 95% credible intervals in the parentheses. The initial susceptibilities, estimated at the end of Sep 2018, were computed by adding the total numbers of individuals immunized by the vaccination campaigns in Oct 2018 to the posterior estimates at the end of Oct 2018.

		Model Settings on Vaccination Campaigns			
	Age group	Baseline	Alternative 1	Alternative 2	Alternative 3
Estimated initial susceptibility (%) at end of Sep 2018	<1 year	53.2 (49, 57.5)	54.2 (50, 58.4)	54.2 (50, 58.5)	54.2 (50, 58.5)
	1-4 years	24.9 (20.4, 29.7)	24.9 (20.4, 29.7)	24.9 (20.4, 29.7)	29.9 (25.4, 34.7)
	5-17 years	6.0 (4.1, 7.9)	7.5 (5.1, 9.9)	7.5 (5.1, 9.9)	6.0 (4.1, 7.9)
	18-49 years	6.0 (4.1, 7.9)	7.5 (5.2, 9.9)	7.5 (5.2, 9.9)	7.5 (5.2, 9.9)
	50+ years	6.0 (4.1, 7.9)	6.0 (4.1, 7.9)	6.0 (4.1, 7.9)	6.0 (4.1, 7.9)
Log-likelihood		-255.25	-265.52	-255.25	-257.42
Relative error of total number of cases over the outbreak	<1 year	0.39%	-11.96%	-11.56%	-17.91%
	1-4 years	-0.04%	-7.80%	-6.90%	-8.07%
	5-17 years	-4.13%	14.38%	0.33%	1.84%
	18+ years	-4.70%	7.24%	5.97%	7.95%
	All ages	-1.79%	-0.65%	-3.48%	-4.25%
Root-mean-square-error (RMSE), over Oct 2018 – July 2019	<1 year	1.74	1.86	1.80	2.55
	1-4 years	8.72	8.13	8.17	7.70
	5-17 years	3.91	5.27	3.00	5.10
	18+ years	5.08	4.62	4.30	4.25
	All ages	7.31	7.52	5.88	6.29
Correlation, over Oct 2018 – July 2019	<1 year	0.99	1.00	1.00	0.99
	1-4 years	0.95	0.96	0.96	0.97
	5-17 years	0.99	0.97	0.99	0.97
	18+ years	0.97	0.97	0.97	0.97
	All ages	0.99	0.99	1.00	1.00
1-step-head prediction RMSE, over Oct 2018 – Mar 2019	<1 year	4.37	4.46	4.40	4.60
	1-4 years	17.13	17.34	17.35	25.12
	5-17 years	8.27	8.39	8.37	8.50
	18+ years	4.34	4.93	4.93	5.06
	All ages	27.79	28.23	28.16	35.02

Fig. S1. Schematic of the measles transmission model. Measles transmission model follows the susceptible (S), exposed (E) and latently infected, infectious (I), and recovered (R) and/or immunized SEIR dynamics and includes 5 age-groups as indicated by the subscripts (i.e., <1, 1-4, 5-17, 18-49, and 50+ year-olds, respectively) and a group (M) for infants with maternal immunity. Black solid arrows show the disease-related processes; grey solid arrows show the demographic processes including birth (horizontal), aging (vertical), and death (tilted). Black dashed arrows show processes related to the routine 2-dose measles vaccination where susceptible individuals are vaccinated at ages 1 and 5 and move to the respective immune groups. Red dotted arrows show processes related to vaccination of susceptible individuals under 18 during the vaccination campaigns.

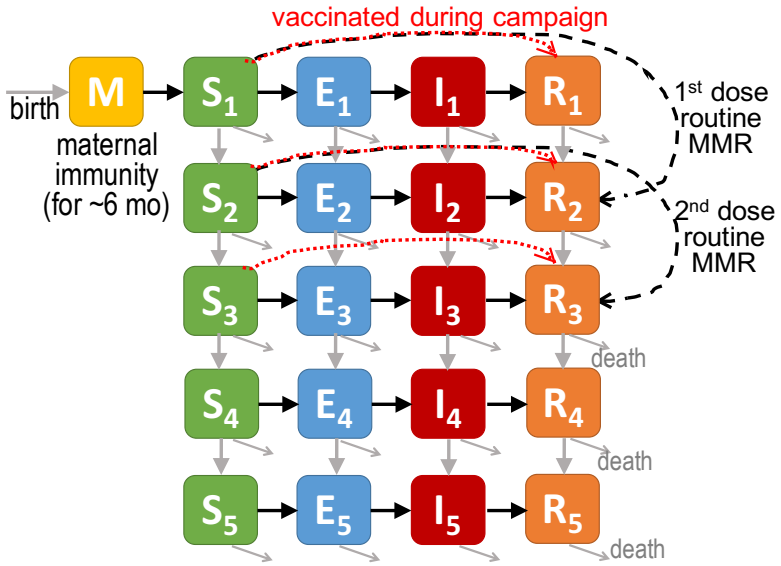
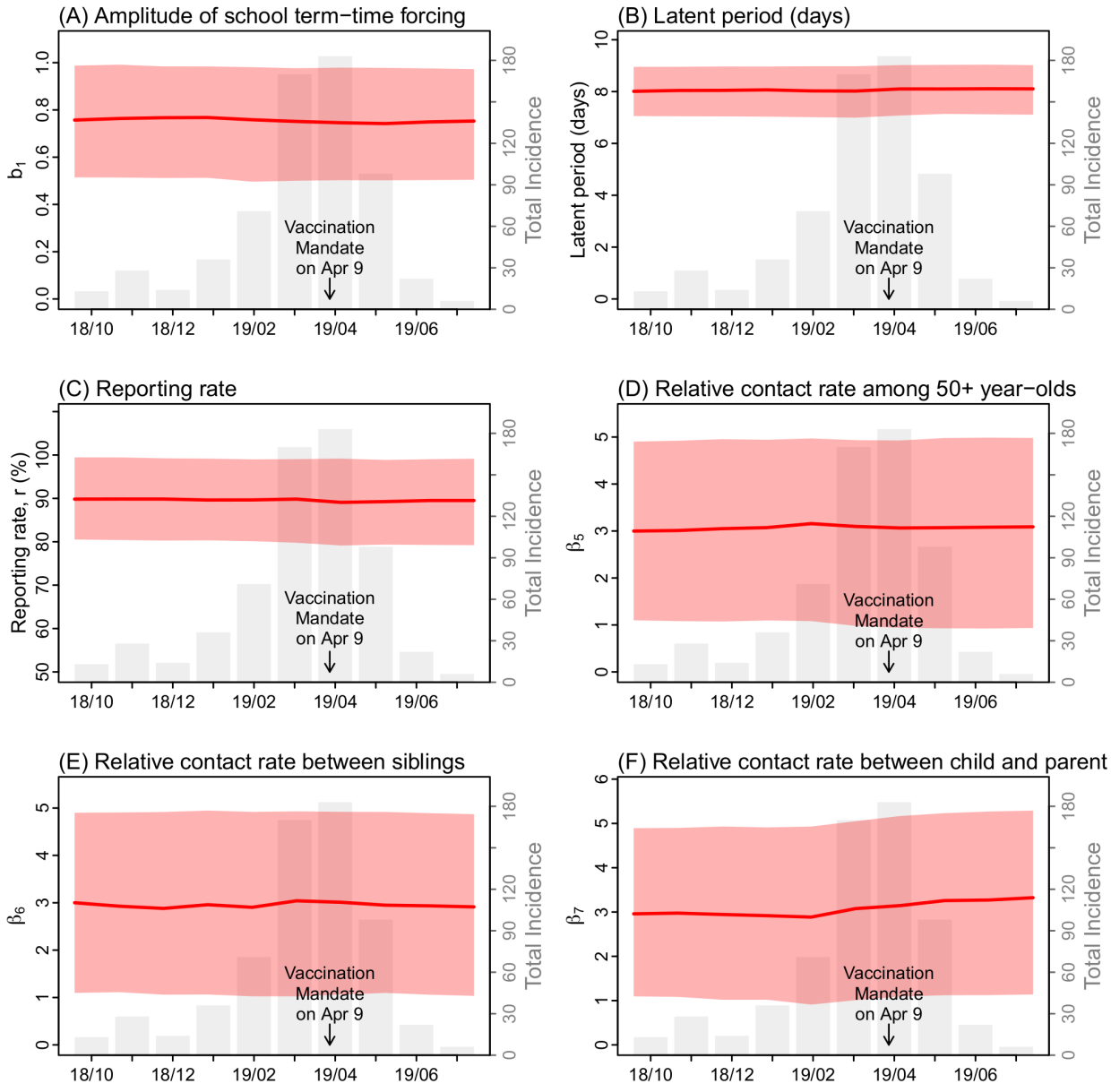
Fig. S2. Estimates of model parameters not listed in Fig. 4: (A) amplitude of school term-time forcing, (B) latent period, (C) reporting rate, (D) relative contact rate among 50+ year-olds, (E) relative contact rate between 1-4 and 5-17 year-olds (i.e. sibling interactions), and (F) relative contact rate between 18-49 and 1-4 or 5-17 year-olds (i.e. parent-child interactions). Red lines and surrounding areas (y-axis on the left) show the mean and 95% credible intervals of estimates pooled over all 10 model-filter runs (100,000 model realizations in total) made at the end of each month from Oct 2018 to July 2019. For comparison, the grey bars (y-axis on the left) show monthly incidence for all ages. Note that m_1 and m_2 are not shown as both optimal priors are the value 1 (Table S1).